Morphology "Phase Diagram" of the Hydrous Alumina Coating on TiO$_2$ Particles during Aqueous Precipitation

Hai-Xia Wu, Ting-Jie Wang,* and Yong Jin

Department of Chemical Engineering, Tsinghua University, Beijing 100084, China

The morphology of the hydrous alumina coating on TiO$_2$ particles from aqueous precipitation at different pHs and temperatures was studied, and a "phase diagram" was obtained. Al$_2$(SO$_4$)$_3$ solution was the coating reagent, and NaOH solution was the precipitant reagent. The effect of pH and temperature on the hydrolysis of Al^{3+}, the size and structure of the OH−Al species, and the coating morphology were investigated. Four kinds of coating morphologies were observed: dotted coating, film coating, floccule coating, and flake coating. When the pH was lower than the isoeletric point of the TiO$_2$ particles (pH 4.1), there was dotted coating. When the pH was higher than the isoeletric point and with increasing pH and temperature, the hydrous alumina coating changed from a uniform and continuous amorphous film coating to a loose floccule coating, then to a flake coating.

1. Introduction

The synthesis of composite particles consisting of a core particle coated with a functional shell has opened new promising directions for advanced materials. The shell can protect the particles from undesirable interactions with the environment and improve the optical, magnetic, conductive, adsorptive, sinterability, and surface reactive properties of the dispersed particles to meet special requirements.[1,2] Various methods[3−5] to achieve uniform coatings on dispersed inorganic or organic particles have been reported in the literature. Precipitation coating in an aqueous solution is one of the most common processes.[6]

The structure and morphology of the coated film are very important in applications.[5,7] They determine the electrical, magnetic, mechanical, and diffusive properties. For example, a nonuniform coating on a ceramic particle has resulted in different sintering rates, leading to residual stress in the coating layer and causing cracks in the ceramic.[7−9]

An alumina coating of the particles has been used in many fields, such as ceramics,[7−9] battery materials,[10,11] phosphors,[2,12] magnetic materials,[13,14] and pigments.[15,16] The particles coated with alumina behave in some ways that are characteristic of alumina. A layer of alumina oxide coating can increase the amount of −OH groups on the particle surface, which can improve the dispersibility of the particles in aqueous solution and provide more active sites for further organic modification.[17]

Aluminum oxide and hydrous alumina have many different structures, which can give many different properties to coated particles. It was reported that the structure of the alumina coating on a titanium dioxide pigment varied with the pH, i.e., alumina precipitated under an acidic condition was amorphous, while alumina precipitated under a basic condition was crystalline, or boehmite under special conditions.[18,19]

In this work, the morphology phase diagram of the hydrous alumina coating on TiO$_2$ particles was investigated. The morphology transitions of the hydrous alumina coating with changes in the operation conditions were also studied.

2. Experimental Section

2.1. Reagents. Commercial TiO$_2$ particles from the sulfate process, in which TiO$_2$ particles were produced from the hydrolysis of TiOSO$_4$ and subsequent calcinations, were used. The TiO$_2$ particles have the rutile structure, are 300 nm in mean diameter, are and nonporous, and have a BET surface area of 6.54 m^2/g. Other chemicals used in the experiments are analytical reagents (AR) grade.

2.2. Coating Operation. The experiments were carried out in a flask with the temperature and pH measured on line with a thermometer and a pH meter, respectively. The TiO$_2$ particles, at a concentration of 50 g/L, were dispersed in deionized water by continuous ultrasonic treatment for 30 min before the coating. Then, 0.3 mol/L of Al$_2$(SO$_4$)$_3$ solution and 1 mol/L NaOH solution were titrated into the TiO$_2$ suspension simultaneously. The TiO$_2$ suspension was stirred strongly and adjusted to a set pH by controlling the titrating speed of the NaOH solution, while the titrating speed of the Al$_2$(SO$_4$)$_3$ solution was kept constant. The temperature was controlled by a constant-temperature bath. After titration, the suspension was aged for 2 h with stirring. Then, coated TiO$_2$ particles were filtered and washed repeatedly, until SO$_4^{2−}$ was no longer detected using a BaCl$_2$ solution, and dried at 120 °C for 12 h. The temperature was investigated in the range of 0−80 °C, and the pH was in the range of 4−10.

2.3. Aging Operation. In the aging process, the effect of temperature and pH on the coating morphology was studied.

2.3.1. Temperature Effect. For the coating process at pH 5 and 20 °C, when the titration was completed, the temperature was increased gradually using a water bath to 80 °C in 30 min. Thereafter, the suspension was aged at pH 5 and 80 °C for 2 h. Samples were taken during the aging process every 10 min.

For the coating process at pH 9 and 80 °C, when the titration was completed, the temperature was decreased using an ice bath to 10 °C in 10 min. Thereafter, the suspension was aged at pH 9 and 10 °C for 2 h. Samples were taken during the aging process every 10 min.

2.3.2. pH Effect. For the coating process at pH 5 and 60 °C, when the titration finished, the pH was adjusted to 10 by adding NaOH solution with a peristaltic pump. Thereafter, the suspension was aged at pH 10 and 60 °C for 2 h. Samples were taken during the aging process every 10 min.

For the coating process at pH 10 and 60 °C, when the titration finished, the pH was adjusted to 5 by adding H$_2$SO$_4$ solution with a peristaltic pump. Thereafter, the suspension was aged at pH 5 and 60 °C for 2 h. Samples were taken during the aging process every 10 min.

* Corresponding author. Tel.: +86-10-62788993. Fax: +86-10-62772051. E-mail: wangtj@mail.tsinghua.edu.cn.

Table 1. Al(OH)$_3$ Gel Structure under Different Conditions

sample	precipitation		aging		crystal structure
	T (°C)	pH	T (°C)	pH	
a	60	6.0	60	6.0	amorphous
b	60	6.0	60	9.0	boehmite
c	60	9.0	60	6.0	boehmite
d	60	6.0	80	6.0	boehmite
e	80	6.0	60	6.0	boehmite

2.4. Blank Experiments. Al$_2$(SO$_4$)$_3$ solution (0.3 mol/L) and NaOH solution (1 mol/L) were titrated simultaneously into 100 mL of deionized water with peristaltic pumps at the pHs and temperatures listed in Table 1. After 2 h of aging, the Al(OH)$_3$ gel was filtered and washed repeatedly, until SO$_4^{2-}$ was no longer detected using a BaCl$_2$ solution, and dried at 120 °C for 12 h.

2.5. Film Characterization. The morphology and structure of the hydrous alumina coating on the TiO$_2$ particles were examined by high-resolution transmission electron microscopy (HRTEM, JEM-2011, JEOL Co., Japan). Samples for HRTEM inspection were dispersed in an ethanol solution by an ultrasonic treatment for 30 min.

The film structure was checked by X-ray diffraction (XRD, D/max-RB, Japan), at a beam voltage of 40 kV, using Cu Kα radiation with a monochromator and a small glancing angle fixed at 2θ.

3. Results and Discussion

It was reported that the temperature, pH, coating reagent concentration, core particle concentration, and particle surface characteristics are all critical parameters in precipitation coating processes.[20] The pH and temperature affect the "hydrolysis−polymerization−precipitation" process of the coating reagent, as well as the coating morphology. A high pH environment speeds up the hydrolysis of Al^{3+}, and more multinuclear OH−Al species are formed compared with the situation at low pH.[21] The number of Al^{3+} ions in an OH−Al species depends on the pH and Al^{3+} concentration, and the structure of the OH−Al species depends on the conditions, e.g., concentration of Al^{3+}, temperature, and stirring strength.[22] The pH also affects the protonation and deprotonation reactions on the core particle surface.[23] Here, the pH and temperature were investigated, and the other parameters were fixed.

3.1. Effect of −OH on the Particle Surface. In our previous work, it was shown that the hydrous alumina coating on TiO$_2$ particles is produced through the collision and condensation of −OH groups on the core particle surface and OH−Al species,[24] and the −OH groups on the particle surface provide protons to trigger the condensation of OH−Al species. The ζ-potential of the TiO$_2$ particles varies with the pH, which indirectly reflects the amount of −OH groups on the particle surface that could provide protons. When the −OH groups can easily provide protons, the particles carry a negative charge; when it is difficult for the −OH groups to provide protons and easily accept protons, the particles carry a positive charge. Thus, at different pH, the ζ-potential reflects the different capacities of the TiO$_2$ particle surfaces to provide or accept protons.

When the pH was lower than the isoelectric point (pH 4.1), the TiO$_2$ particles carried a positive charge,[24] which reflected that the capacity of −OH groups providing protons was very weak, and the condensation between the OH−Al species and the −OH groups on the particle surface seldom occurred. Since only a few −OH groups could provide protons, the condensed OH−Al species were usually isolated and the neighboring
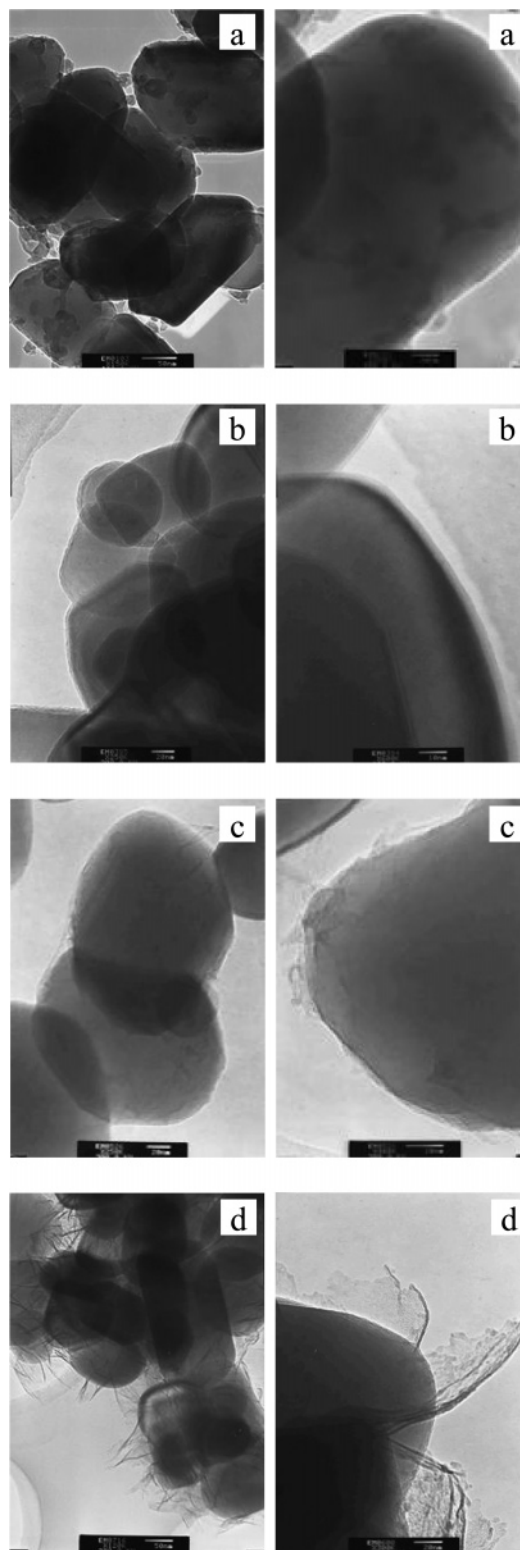

Figure 1. HRTEM images of typical coating morphologies: (a) dotted coating, (b) film coating, (c) floccule coating, and (d) flake coating.

condensed OH−Al species hardly condensed each other, forming a dotted coating of nanoparticles on the surface, as shown in Figure 1a.

When the pH was higher than the isoelectric point, the TiO$_2$ particles carried a negative charge;[24] their surface was easy to provide protons and facilitated the condensation between the OH−Al species and the −OH groups on the particle surface. Since a large amount of −OH groups on the particle surface could provide protons at the higher pH, there were many OH−
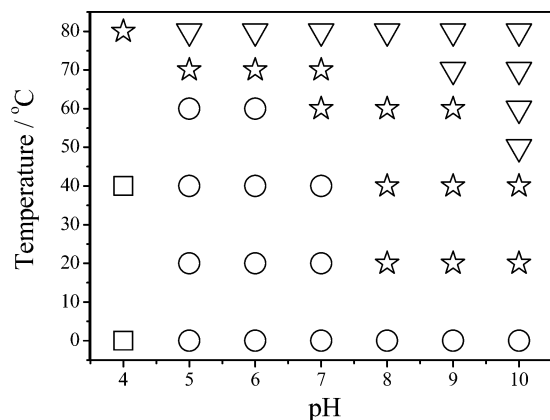
Figure 2. Morphology phase diagram at different pHs and temperatures: (a) □, dotted coating; (b) ○, film coating; (c) ☆, floccule coating; and (d) ▽, flake coating.

Al species that condensed with the −OH groups on the particle surface, and the neighboring condensed OH−Al species were easy to condense each other, forming a continuous film coating, as shown in Figure 1b.

With less −OH groups on the core particle surface, the result is easier to cause homogeneous nucleation, i.e., a dotted coating of nanoparticles. With more −OH groups on the core particle surface, the result is easier to cause heterogeneous nucleation, e.g., film coating.

3.2. Morphology Phase Diagram. The particle coating experiments were carried out at different temperatures of 0−80 °C and pHs of 4−10. The morphology of coated particles was characterized by HRTEM. It was observed that the coating morphologies can be divided into four kinds.

The first is dotted coating with nanoparticles adhering on the core particle surface, and the nanoparticles are usually isolated, which is shown in Figure 1a. The second is film coating with a uniform and continuous layer that tightly binds to the core particle surface with a film thickness of several nanometers, shown in Figure 1b. The third is floccule coating with a loose layer, which covers the core particle surface nonuniformly, shown in Figure 1c. The fourth is flake coating with flakes almost vertically coated on the core particle surface, which is shown in Figure 1d.

Figure 2 shows the morphology phase diagram for the conditions studied, with the four kinds of morphology marked with different symbols. Besides dotted coating, the other three kinds were produced when the pH was higher than the isoeletric point 4.1. When the pH was lower than the isoeletric point, the number of −OH groups on the particle surface that could provide protons was small and the condensation with the OH−Al species hardly occurred, and homogeneous nucleation or the dotted coating was preferred.

When the pH was higher than the isoeletric point, the number of −OH groups on the particle surface that could provide protons was large and the condensation with the OH−Al species easily occurred, and heterogeneous precipitation was preferred. The coating morphology mainly depends on the sedimentation speed and the directed growth speed of the OH−Al species.[25] When the sedimentation speed was higher than the directed growth speed, a continuous and amorphous film coating was produced because of the random condensation of OH−Al species and −OH groups on the particle surface. When the directed growth speed was higher than the sedimentation speed, a loose floccule or flakelike coating was produced because of the directed condensation.

When the temperature was low, the temperature and the directed growth speed had less effect on the precipitation process. Since the sedimentation speed was high, the precipitation mainly depended on the random condensation among the −OH groups and OH−Al species, and a uniform and continuous film coating was produced. Since the sedimentation speed of the OH−Al species was much higher than the directed growth speed, a uniform and continuous film coating was still preferred even at high pH.

When the temperature was in the middle range, the sedimentation speed and the directed growth speed of the OH−Al species were about the same. At low pH, the OH−Al species had a small size, random sedimentation dominated the precipitation process, and a uniform and continuous film coating was produced. At high pH, the OH−Al species were large and had a certain shape, and their sedimentation led to a loose floccule or flakelike coating.

When the temperature was high, the directed growth speed of the OH−Al species dominated the precipitation process regardless of the pH and size of the OH−Al species, which resulted in a directed growth and led a flakelike coating.

3.3. Morphology Transition. The transition in the morphology was investigated in the aging process. When the temperature was increased from 20 to 80 °C at a fixed pH, the coating morphology changed from a uniform and continuous film, to a loose floccule, and then to a flake, which is shown in Figure 3.

In the aging process, a high temperature sped up the dissolution and sedimentation of the OH−Al species, and a self-assembly process occurred that led to a more stable structure with lower energy. The OH−Al species in the uniform and continuous film were dissolved and self-assembled, and the film became a loose floccule. When the temperature was high enough, flakes with an ordered microstructure formed on the particle surface.

However, when the process was reversed, i.e., coating at a high temperature and aging at a low temperature, the flake could not be changed to a floccule or film, as shown in Figure 4. When the coating process was performed at high pH and high temperature, the OH−Al species precipitated preferentially in a certain direction and formed a more ordered flake that was more stable, and the OH−Al species could not be changed to the disordered states of a film. The morphological transition was also investigated when the aging pH was increased from 5 to 10 at 60 °C. The morphology changed from a film to a flake during the aging process.

When the aging pH was increased, the number of Al^{3+} in an OH−Al species and the OH−Al species size increased. The OH−Al species of small size dissolved from the particle surface in the solution forming large ones, which precipitated on the particle surface spontaneously in a dynamic equilibrium of dissolution and sedimentation. When the aging temperature was not very low, a larger OH−Al species size showed a more obvious self-assembly phenomena, which changed the disordered OH−Al species in the film into the ordered structure in the flake. Thus, when the aging pH was increased, the coating morphology also changed from a film, to a floccule, and then to a flake. However, when the aging pH was decreased from 10 to 5, the flake hardly changed into a floccule or a film, because the flake was more stable than the floccule or film. Therefore, the transition of film to flake is irreversible.

3.4. Comparison with the Al(OH)₃ Gel. Figure 5 shows the crystal structure of $Al(OH)_3$ gels precipitated under the different conditions in Table 1. The X-ray diffraction patterns of the $Al(OH)_3$ gels show mainly boehmite. Amorphous Al-
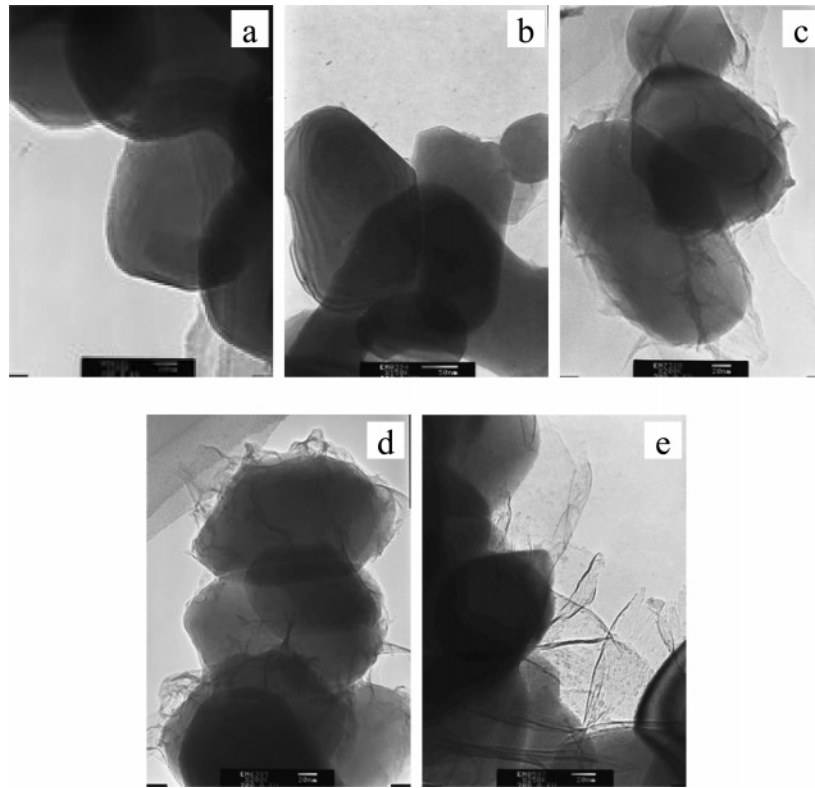
Figure 3. Morphology transition in the aging process (pH 5): (a) before aging (coating at pH 5, 20 °C); (b) sample a aging 10 min (20→70 °C); (c) sample b aging 10 min (70→80 °C); (d) sample c aging 10 min (80 °C); and (e) sample d aging 10 min (80 °C).
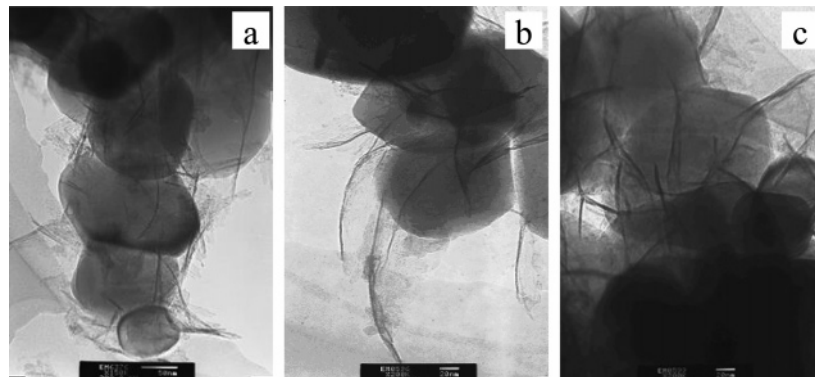

Figure 4. Morphology transition in the aging process (pH 9): (a) before aging (coating at pH 9, 80 °C); (b) sample a aging 10 min (80→10 °C); and (c) sample b aging 10 min (10 °C).
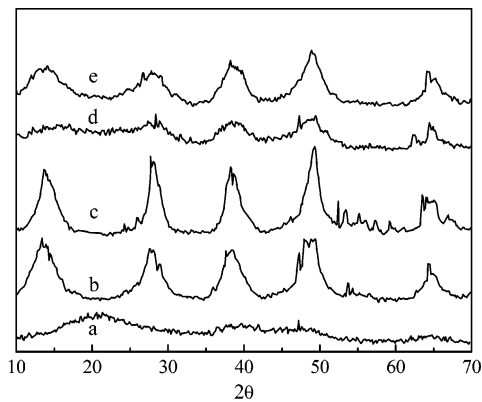

Figure 5. X-ray diffraction pattern of Al(OH)$_3$ gel under different conditions; a, b, c, d, and e conditions are listed in Table 1.

(OH)$_3$ gel could be obtained only when the precipitation and aging were at a low temperature and pH, and it could be changed to boehmite when the pH or temperature was high. How-

ever, the boehmite gel could not be converted to the amorphous form when the pH and temperature were low in the aging process.

The gel structure change agrees well with the morphology transition in the particle coating process. At a high pH or temperature, in the precipitation or aging, boehmite Al(OH)$_3$ gels formed, while in coating or aging, the coating morphology with a floccule or a flake formed. At a low pH and temperature, in gel precipitation and aging, amorphous Al(OH)$_3$ gels formed, while in coating and aging, the coating morphology with a continuous and uniform film formed.

In gel precipitation or coating, the temperature affects the direction and growth speed of the OH−Al species, while in the aging process, the temperature affects the self-assembly of the OH−Al species. Both result in the formation of stable boehmite Al(OH)$_3$ gels or a floccule/flake coating. A high pH brings about a large size of the OH−Al species, which facilitates the formation of boehmite Al(OH)$_3$ gels or a floccule/flake coating.

4. Conclusion

An analysis of the coating process shows that the −OH groups on a particle surface affect the precipitation and condensation of the OH−Al species and determine whether homogeneous or heterogeneous nucleation dominates in the precipitation coating process. The morphology under different conditions was obtained. Four kinds of coating morphology were observed at different pHs and temperatures: a dotted coating with nanoparticles adhering to the core particle surface, a film coating with a uniform and continuous layer of several nanometers thickness, a floccule coating with a nonuniform loose layer, and a flake coating with flakes that are almost vertically coated on the surface. During coating or aging, a floccule or a flake coating is produced at high pH or temperature; while at low pH and temperature, a film coating is produced. A high temperature speeds up the directed growth and self-assembly of the OH−Al species, and a high pH produces large OH−Al species, and a floccule/flake coating is produced.

Literature Cited

(1) Nakamura, H.; Yoshinaga, M.; Nagashima, S.; Kato, A. Preparation of SiC particles coated with alumina hydrate: effect of reaction condition on particle coalescence. *J. Eur. Ceram. Soc.* **1996**, *16*, 1329.

(2) Cui, H. T.; Hong, G. Y.; You, H. P.; Wu, X. Y. Coating of Y₂O₃: Eu³⁺ particles with alumina by a humid solid-state reaction at room temperature. *J. Colloid Interface Sci.* **2002**, *252*, 184.

(3) Zhang, J. X.; Gao, L. Q. Nanocomposite powders from coating with heterogeneous nucleation processing. *Ceram. Int.* **2001**, *27*, 143.

(4) Ding, D. Y.; Rao, J. C.; Wang, D. Z.; Ma, Z. Y.; Geng, L.; Yao, C. K. Sol−gel alumina coatings for whisker reinforced metal matrix composites. *Mater. Sci. Eng., A* **2000**, *279*, 138.

(5) Bertrand, G.; Filiatre, C.; Mahdjoub, H.; Foissy, A.; Coddet, C. Influence of slurry characteristics on the morphology spray-dried alumina powders. *J. Eur. Ceram. Soc.* **2003**, *23*, 263.

(6) Haq, I.; Matijevic, E. Preparation and properties of uniform coated inorganic colloidal particles. *J. Colloid Interface Sci.* **1997**, *192*, 104.

(7) Nakamura, H.; Chen, Y. F.; Kimura, K.; Tateyama, H.; Hirosue, H. The effect of the reaction conditions on the morphology of coating layers of alumina hydrate on silicon carbide whiskers. *Powder Technol.* **2001**, *117*, 270.

(8) Prabhakaran, K.; James, J.; Pavithran, C. Surface modification of SiC powders by hydrolyzed aluminum coating. *J. Eur. Ceram. Soc.* **2003**, *23*, 379.

(9) Kato, A.; Nakamura, H.; Tamari, N.; Tanaka, T.; Kondo, I. Usefulness of alumina-coated SiC whiskers in the preparation of whisker-reinforced alumina ceramics. *Ceram. Int.* **1995**, *21*, 1.

(10) Myung, S. T.; Izumi, K.; Komaba, S.; Sun, Y. K.; Yashiro, H.; Kumagai, N. Role of alumina coating on Li−Ni−Co−Mn−O particles as positive electrode material for lithium-ion batteries. *Chem. Mater.* **2005**, *17*, 3695.

(11) George, T. K. F.; Chena, J. G.; Kumarb, T. P. Carboxylate-alumoxanes as precursors for alumina coatings to enhance the cyclability of LiCoO₂. *J. Power Sources* **2005**, *146*, 250.

(12) Lee, R. Y.; Kim, S. W. Low voltage cathodoluminescence properties of ZnS:Ag and Y₂SiO₅:Ce phosphors with surface coatings. *J. Lumin.* **2001**, *93*, 93.

(13) Núñez, N. O.; Tartaj, P.; Morales, M. P.; Pozas, R.; Ocaña, M.; Serna, C. J. Preparation, characterization, and magnetic properties of Fe-based alloy particles with elongated morphology. *Chem. Mater.* **2003**, *15,* 3558.

(14) Guo, Y. H.; Zhang, Y. Preparation and surface chemistry characteristics of pure and coated acicular α-FeOOH particles. *Mater. Chem. Phys.* **1997**, *47*, 211.

(15) Yuan, F. L.; Peng, H.; Yin, Y.; Chunlei, Y.; Ryu, H. Preparation of zinc oxide nanoparticles coated with homogeneous Al₂O₃ layer. *Mater. Sci. Eng., B.* **2005**, *122*, 55.

(16) Qin, C.; Wang, T. J.; Jin, Y. Nanoscale film coating of alumina on TiO₂ particles. *J. Process Eng. (Chinese)* **2002**, *2*, 87.

(17) Lin, Y. L.; Wang, T. J.; Jin, Y. Surface characteristics of hydrous silica coated TiO₂ particles. *Powder Technol.* **2002**, *123*, 196.

(18) Edward, C. M. Titanium dioxide pigment and process making same. U.S. patent 4,022, 636, 1977.

(19) Thomas, F. S.; Woburn, M. Nongelling Titania pigments. U.S. patent 3,523,810, 1966.

(20) He, Y. X. Ceramic composites through solution precipitation coating. Ph.D. Dissertation, University of California, Berkeley, CA, 1998.

(21) Lu, X. Q.; Chen, Z. L.; Yang, X. H. Spectroscopic study of aluminium speciation in removing humic substances by Al coagulation. *Water Res.* **1999**, *33*, 3271.

(22) Bi, S. P.; Wang, C. Y.; Cao, Q.; Zhang, C. H. Studies on the mechanism of hydrolysis and polymerization of aluminum salts in aqueous solution: correlations between the "core-links" model and "cage-like" keggin-Al₁₃ model. *Coord. Chem. Rev.* **2004**, *248*, 441.

(23) Tombácz, E.; Libor, Z.; Illés, E.; Majzik, A.; Klumpp, E. The role of reactive surface sites and complexation by humic acids in the interaction of clay mineral and iron oxide particles. *Org. Geochem.* **2004**, *35*, 257.

(24) Wu, H. X.; Wang, T. J.; Jin, Y. Film coating process of hydrated alumina on TiO₂ particles. *Ind. Eng. Chem. Res.* **2006**, *45*, 1337.

(25) Shen, Z.; Zhao, Z. G.; Wang, G. T. *Colloid and Surface Chemistry;* Chemistry Industry Press: Beijing, China, 2004.